

Applying Computer Simulation in Improving Heat Treating Condition of Thin High-Carbon Steel Parts

Thanaporn KORAD*, Mana POLBOON, Niphon CHUMCHERY and John PEARCE

*National Metal and Materials Technology Center, Klong Luang,
Pathumthani 12120 Thailand*

Abstract

The study was carried out using COSMOSFlowWorks® to predict heat treatment conditions for AISI 1085 high-carbon steel sheet that is used to produce automotive parts that require wear resistance and stiffness resulting from controlled moderately high hardness levels. To achieve such properties, flat high-carbon steel parts need to be hardened to produce acicular matrix structures, and the most suitable heat treatment process to harden thin parts without distortion is austempering. In producing hard and stiff thin section parts in this company study the austempering process was performed by soaking at 830°C and then quenching in a NaCl salt bath at 335°C. In production hardness testing is performed to ensure that parts have microstructures of lower bainite and martensite instead of upper bainite. To reduce distortion without any effect on hardness, modified austempering conditions were determined using temperature prediction from commercial computational analysis software. This enabled a more suitable production line practice for the production of austempered parts without distortion whilst avoiding reduced hardness.

Key words: Austempering, Hardening, High carbon steel, Bainite structure

Introduction

Austempering is a heat treatment practice that enables the production of hard-acicular-structures in medium-to-high carbon steels without distortion. Conventional austempering ensures the formation of fully bainitic or mixed bainite-martensite microstructures in steel by controlling the cooling conditions of parts with respect to their design and section size in relation to the Time-Temperature-Transformation characteristics of the steel.

Thin section steel parts for automotive applications are made from AISI 1085 high-carbon steel (Table 1) and require suitable hardening heat treatment to provide sufficient strength and stiffness according to Tu et al. ⁽⁶⁾. Typically, austempering practice helps in achieving high strength with good ductility and toughness by evolving a predominantly bainitic microstructure in the steel according to Saxena et al. ⁽⁴⁾. The parts require specified tensile strengths of above 1,350 MPa, but only hardness testing can be used to qualify such parts. The specified hardness range for the steel parts in this study is 420-520 HV. Most of the parts can satisfy this requirement, but 5-10% of these parts are rejected

due to low hardness of 400-420 HV from structures of upper bainite possibly caused by low cooling rate. To ensure sufficient hardness levels in heat treated parts, production is operated at high cooling rate to produce hard bainitic structures; however such rapid cooling can cause some heat treated parts to be rejected because of distortion. Austempering is therefore controlled to produce mixed lower bainitic-martensitic structures instead of the lower hardness upper bainite-ausferrite structures according to Chakraborty et al. ⁽²⁾, but this must be balanced against preventing distortion.

The first part of austempering practice is complete austenitisation at sufficiently high temperature to enable complete solution of all carbides and to homogenize the austenite. The steel is then quenched in a salt bath or fluidized bed to transform the austenite to controlled amounts of bainite and martensite. In the current study the production line is continuous consisting of austenitizing at 830°C, quenching into a salt bath at 335°C and then cooling in water bath at 40°C.

Figure 1 shows the isothermal transformation characteristics of a nominal

*Corresponding author Tel: +66 2564 6500 ext. 4030; Fax: +66 2564 6336; E-mail: thanapk@mtec.or.th

0.8wt% C steel. Above the nose of the curve (550°C) the austenite will transform to relatively soft pearlite. Below the nose at temperatures down to around 250°C the austenite will transform to bainite which consists of acicular ferrite containing very fine precipitated carbides, and which is harder and stronger than pearlite. Martensite forms from any residual austenite on cooling after isothermal treatment in the salt bath; the amount of residual austenite and hence martensite depends on the holding time in the salt bath.

Treatment in the range 450°C down to 350°C will normally result in upper bainite, treatment from 350°C down to 250°C giving lower bainite. Upper bainite has a lower hardness than lower bainite. Transformation to different microstructures, i.e. martensite, lower bainite or upper bainite, or mixed structures, results in different volumetric changes giving rise to varying degrees of tendency towards shape distortion of heat treated parts.

Table 1. Chemical composition of typical AISI 1085 compared with a random analysis check on the examined parts.

Wt%	C	Si	Mn	P	S
AISI1085	0.80-0.90	0.15-0.30	0.70-1.00	< 0.04	< 0.05
Sample	0.83	0.18	0.43	0.01	0.006

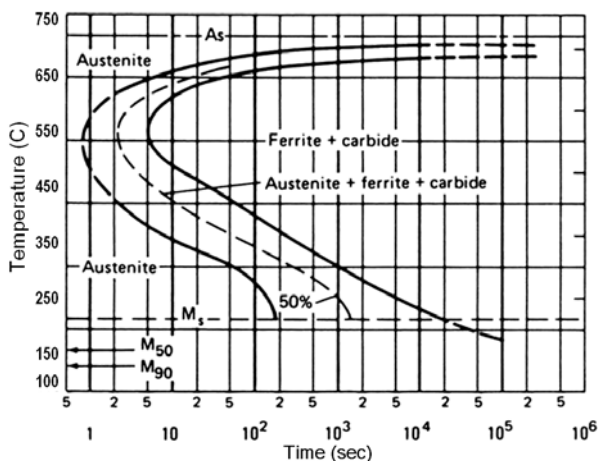


Figure 1. TTT diagram for AISI 1080 steel (0.75-0.85%C), quenching from austenitizing to austempering temperature typically is within a few seconds ⁽¹⁾.

Materials and Experimental Procedures

This study has examined the microstructures of three austempered thin parts, namely a hose ring clamp with outer diameter of 2.4 mm and thickness of 0.9 mm., a shim plate with thickness of 0.6 mm., and a screen plate with thickness of 1.5 mm. The hose ring clamp was designed as a stiff part while the shim plate and screen plate were designed to have a good wear resistance. All parts need to be hardened since high hardness is required. During mass production, distortion of the parts is the main reason for rejection rather than low hardness. Detail of the austempering process and the controlled parameters are shown in Figure 2, and the geometry of a hose ring clamp (one of the studied parts) is shown in Figure 3.

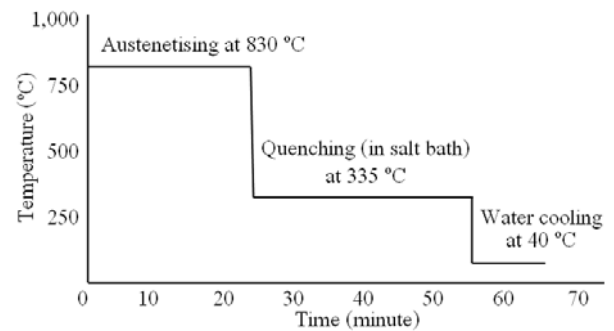


Figure 2. Temperature profile in experiment performed in continuous furnace.

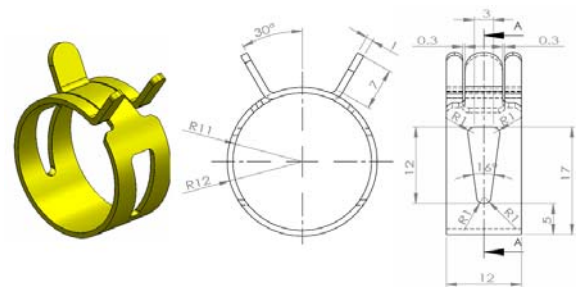


Figure 3. Hose ring clamp, one of three parts which found distortion in the production line.

All three part designs were made from AISI 1085 eutectoid steel using the same heat treatment time and temperature control in spite of their differences in geometry. The manufacturer had previously studied the problem of distortion and decided to adjust the heat treatment condition to “softer austempering” involving a slower cooling rate. The trial resulted in decreased rejects

from distortion, but increased rejection due to unacceptable low hardness levels. The other possible alternative modification considered by the manufacturer was increasing thickness of the raw materials, from 0.9 mm., 0.6 mm., and 1.5 mm. to 1.0 mm., 0.7 mm., and 1.6 mm., respectively. Increasing thickness was studied using flat sheet specimens to verify only microstructure and hardness. However, before applying increased thickness on the production line, the operator wished to perform simulation to study how cooling conditions such as temperature gradient and cooling rate compare to those previously experienced, particularly with regard to problems of distortion and inadequate hardness levels. With this aim COSMOSFlowWorks® is the commercial software that was applied to simulate the austempering conditions.

In this study, the simulated austempering condition was started at 830°C and flow velocity of salt bath was set at 0.001 m/s for the external flow simulation. The austempered solid bodies were set following boundary conditions for AISI 1085 steel such as a density of about 7,400 kg/m³ which was fixed while thermal conductivity and specific heat were variable between 535 to 600 J/kg·K and 15.1 to 26.6 W/m·K, respectively. The software computed using model equations⁽⁶⁾ for the austempered bodies, salt bath and the temperature gradient such as continuity equation (1), momentum equation (2) and energy equation (3) as follows:

$$\frac{\partial \rho}{\partial t} + \frac{\partial}{\partial x_i}(\rho u_i) = 0 \quad (1)$$

$$\frac{\partial \rho u_i}{\partial t} + \frac{\partial}{\partial x_j}(\rho u_i u_j) + \frac{\partial p}{\partial x_i} = \frac{\partial}{\partial x_j}(\tau_{ij} + \tau_{ij}^R) + S_i, \quad i=1,2,3 \quad (2)$$

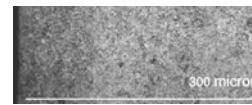
$$\frac{\partial \rho H}{\partial t} + \frac{\partial \rho u_i H}{\partial x_i} = \frac{\partial}{\partial x_i}(u_j(\tau_{ij} + \tau_{ij}^R) + q_i) + \frac{\partial p}{\partial t} - \tau_{ij}^R \frac{\partial u_i}{\partial x_j} + \rho \varepsilon + S_i u_i + Q_{it} \quad (3)$$

Results and Discussion

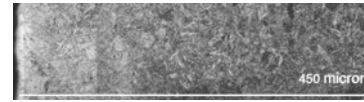
Microstructural examination of parts with the original thickness rejected because of distortion showed that parts produced from the same steel in different thicknesses and austempered under the same conditions could have significantly different microstructures. Some typical microstructures are shown in Figure 4.

The thinnest part, a shim plate having thickness of 0.6 mm exhibited the finest acicular structures (Figure 4 (a)) with HV0.1 hardness

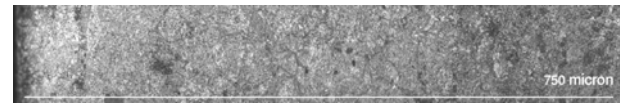
levels of between 538 to 587 HV. The part with a thickness of 0.9, a hose ring, had hardness of between 537 to 597 HV (Figure 4 (b)) while a screen plate, the thickest part at 1.5 mm, had hardness of between 408 to 494 HV (Figure 4 (c)). Figure 5 is the scatter plots between predicted cooling rates and measured hardness levels. Basically testing hardness on thin metal parts has limitations that effect on the measurement accuracy according to Li et al.⁽³⁾. Hence, trendlines and error bars are also added in the plots exhibiting that the increase of the average hardness is a result of increasing the predicted cooling rates.



(a)



(b)

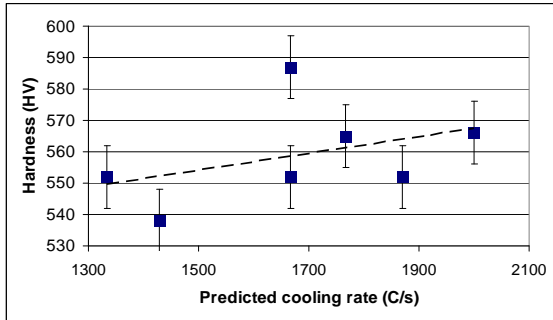


(c)

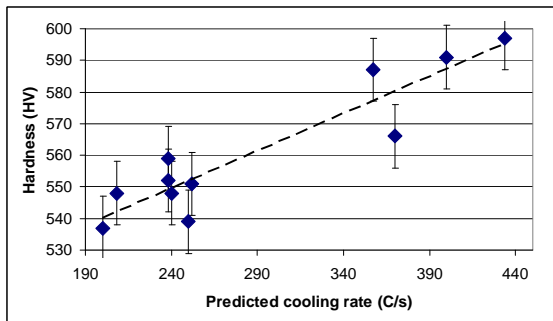
Figure 4. Cross section microstructures of the examined samples from edge to center of (a) shim plate, (b) hose ring clamp and (c) screen plate. Micrographs show uniform acicular and fine structures along the cut surfaces (edge to center) ensuring that the applied soft austempering could result in hardening heat treatment.

By using COSMOSFlowWorks® software, heat flow during quenching in the salt bath was analyzed for each of the three parts to provide data on temperature gradients at different positions of each part. This allowed the cooling rates to be drawn for comparison with suitable cooling curves for austempering practice in the AISI 1085 TTT diagram. The simulated cooling curves from the software calculation show that significant differences exist between the edge and the center areas of each part as well as at the outer and inner edges of the holes in the hose ring and screen plate designs. Figure 6 illustrates different cooling curves resulting in significantly different hardening and residual stress, exhibited from

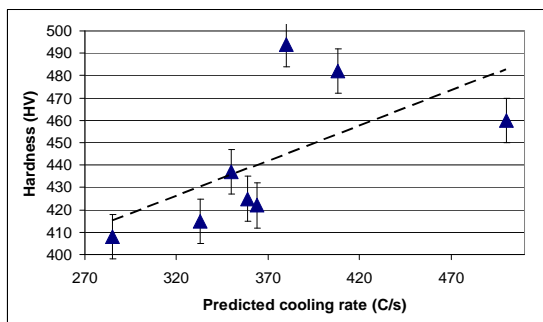
simulation results while raw data from simulation analyzed at 2.8 seconds after quenching is displayed in Figure 7. The data reveals temperature differential of almost 100°C within the part that could give rise to distortion.



(a) Shim plate, predicted cooling rate is 1,330-2,020°C /s.



(b) Hose ring, predicted cooling rate is 200-434°C /s.



(c) Screen plate, predicted cooling rate is 285-504°C /s.

Figure 5. Plots relationship between predicted cooling rates only at the steep stage from austenitizing temperature to austenite start (723°C) and hardness checks from different positions in (a) shim plate (b) hose ring clamp and (c) screen plate.

Cooling was then simulated after allowing for increased sheet thickness in each part. It was seen that cooling rate was less variable when sheet thickness was increased as indicated by the data in Figure 8. By following the same analysis steps on each part, the cooling curves

from the simulation for thicker raw material are illustrated on the TTT diagram (Figure 9) suggesting that the modified cooling conditions would be suitable for austempering of AISI 1085 before actual application on the production line.

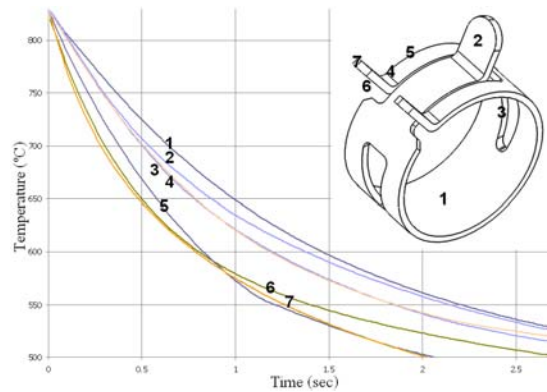


Figure 6. Plots of cooling curve simulated from COSMOSFlowWorks® analyzing on sections that possibly cause distortion happened on hose ring clamp.

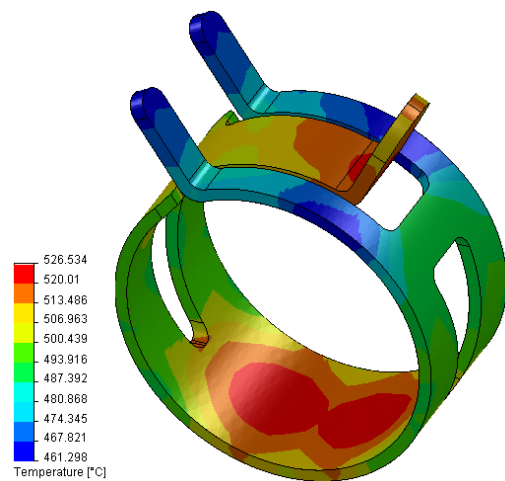


Figure 7. Simulated data of temperature change in hose ring clamp during austempering, comparing between the fastest cooling area and the thick section.

The simulation experiment showed that the redesign of the parts by increasing thicknesses could reduce the differences between the fastest and slowest cooling regions in each part. Equally it was predicted that this modified cooling would be suitable for AISI 1085 austempering practice.

Simulation helped the manufacturer to redesign the parts with increasing thickness. This

was reinforced by trial samples to check microstructural features and hardness. Bainitic and martensitic structures in the thicker parts were similar to those in the previous thinner sheet designs; the average hardness levels were slightly lower, but no distortion problems were experienced in the trial production batch.

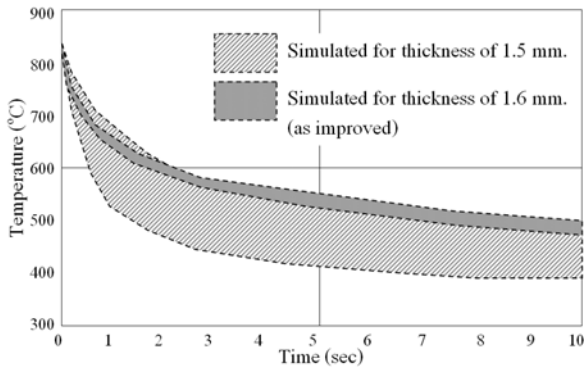


Figure 8. Comparing between before and after increasing thickness aiming to reduce distortion on screen plate.

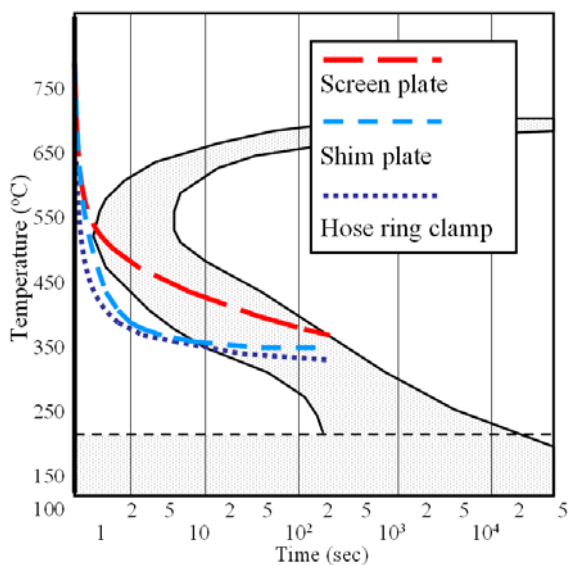


Figure 9. Illustration of simulated data plotted to show temperature profile for austempering the studied part after the design improvement.

Conclusions

The computational analysis simulation technique of heat flow analysis showing temperature gradient data assists producers in the redesign of metal parts to meet exacting hardness and mechanical property requirements without the dangers of part shape distortion that can result

from excessive temperature differences within a part during quenching treatments for hardening.

References

1. American Society for Metals. (1977). *Atlas of isothermal transformation cooling transformation diagrams*. : ASM.
2. Chakraborty, J., Bhattacharjee, D. & Manna, I. (2008). Austempering of bearing steel for improved mechanical properties. *Scripta Mater.* **59(2)**: 247-250.
3. Li, H. & Zhou, X. (2007). The Application and Effects of Thin Sheet Hardness Reference Materials without Aging Effect. In: *Proceedings of HARDMEKO 2007 Recent Advancement of Theory and Practice in Hardness Measurement*. November 19-21, Tsukuba, Japan: 117-119.
4. Saxena, A., Prasad, S.N., Goswami, S., Subudhi, J. & Chaudhuri, S.K. (2006). Influence of austempering parameters on the microstructure and tensile properties of a medium carbon-manganese steel. *Mat. Sci. Eng. A-Struct* **431(1-2)**: 53-58.
5. Tu, M.Y., Hsu, C.A., Wang, W.H. & Hsu, Y.F. (2008). Comparison of microstructure and mechanical behavior of lower bainite and tempered martensite in JIS SK5 steel. *Mater. Chem. Phys.* **107(2-3)**: 418-425.
6. Zienkiewicz, O.C. & Taylor, R.L. (2000). *Finite element method* (5th ed.). (Vol.3 Fluid Dynamics): Butterworth-Heinemann.